

## AN EVALUATION OF LOCAL SITE EFFECTS ON STRONG GROUND MOTION CONSIDERING MICROLANDFORM AND DEEP SUBSURFACE STRUCTURE

I. OKAWA<sup>1)</sup>, J. SHIBUYA<sup>2)</sup>, M. YAMADA<sup>3)</sup>, K. HAGIO<sup>4)</sup>, M. TOHDO<sup>5)</sup>

<sup>1)</sup> Building Research Institute, Ministry of Construction, Government of Japan,  
Tatehara-1, Tsukuba-shi, Ibaraki-ken, JAPAN

<sup>2)</sup> Tohoku University, Aoba, Aoba-ku, Sendai-shi, Miyagi-ken, Japan

<sup>3)</sup> Waseda University, 17 Kikui-cho, Shinjuku-ku, Tokyo, Japan

<sup>4)</sup> Taisei Corporation, 344-1, Naze-cho, Totsuka-ku, Yokohama, Kanagawa, Japan

<sup>5)</sup> Toda Corporation, 4-6-1, Hatchobori, Chuo-ku, Tokyo, Japan

### ABSTRACT

The surface geological condition is, more or less, taken into account in most seismic structural design provisions or requirements. In view of the shortcoming of the effect of topography in the current seismic design practice, however, a research project was set up for establishing a methodology of local site effect including the topographical effect. We investigated the representative patterns of subsurface topography in urban area of Japan. The topography was roughly classified into four categories, slope, hill, sediment-filled valley, dipping base layer. For slope, the angle and the height of the slope vary with its location. The general tendency and dimensions of each topography were provided for districts. The literature survey was also conducted to obtain the actual behaviors of ground during past earthquakes clearly justifying the topographical effect on earthquake-induced ground motions and the subsequent structural damage. The analytical study was conducted to find the effectiveness of each topography parameters such as angle and heights. A Ricker's wavelet input is used to make problems as simple as possible. In this paper, the dynamic property of soil including topographical effect on seismic motion research and interim analytical results are shown with some considerations found for the final evaluation procedures.

### KEYWORDS

Topography, Ricker's Wavelet, Incident Angle, Slope Angle, Amplification, Sediment-filled Valley, Dipping Base Layer, Damage

### INTRODUCTION

There are many factors to consider in the current seismic design practice of building structures. The soil condition is one of such factors being so complicated to evaluate. The complexity comes from the difficulty in knowing all the properties of surrounding geological environment as well as the uncertainty of earthquake ground motions. The local site effect is mainly evaluated with the amplification in vertical direction at present. A guideline for composing the design earthquake ground motion for buildings was proposed (BRI et al., 1992). In the guideline the soil condition is based on only vertical propagation assumption, although a methodology with topography is implemented. In view of the ground motion implications in recent large

earthquake in Japan, however, a practical method to consider the topographical effect is urgently needed. The research activity presented in this paper is an ongoing project for constructing the practical methodology to evaluate the topographical effect on seismic motion and reflect on seismic design method. This paper mainly introduces the contents of the work.

## SURFACE GEOLOGY AND TOPOGRAPHY IN URBAN AREAS OF JAPAN

The geometrical irregularity in geology is classified into two types. One is the irregularity of surface landform, and the other is the irregularity of interfaces of soil layers. The former includes the slope (cliff), hill, and valley etc. The latter includes the sediment-filled valley, the dipping base layer and horizontal discontinuity of layers due to fault etc.

The representative soil conditions of (1) Slope, (2) Hill, (3) Sediment-filled Valley, and (4) Dipping Base Layer were selected as shown in Fig.1 and examined the distribution of the following parameters for each of the urban areas in Japan.

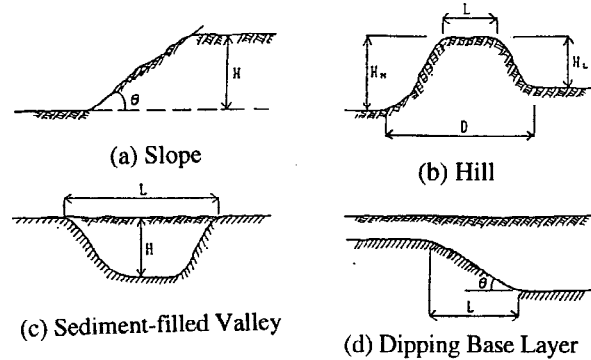


Fig.1 Representative topography

From the survey, average values of simplified topography parameters are summarized for some district of Japan.

Table 1. Average values of simplified topography parameters for areas of Japan

		Tokyo	Osaka	Nagoya	Yokohama	Kawasaki
Slope	$\theta$ (deg)	10	< 5	-	40 - 60	20 - 40
	H (m)	10 - 20	10 - 30	-	5 - 15	5 - 20
Hill	L (m)	100 - 500	< 500	100 - 400	-	-
	H (m)	5 - 10	< 10	5 - 20	-	-
	D (m)	300 - 900	200 - 500	200 - 1300	-	-
Sediment-filled Valley	L (m)	100 - 400	-	vary	-	-
	H (m)	3 - 4	-	5 - 16	-	-
Dipping Base Layer	L (m)	100 - 300	100 - 400	500	-	-
	$\theta$ (m)	< 1	0.2 - 0.6	0.4 - 0.8	-	-

A location has its specific geological structure. Consequently, the seismic motion thus transmitted through such strata has site specific properties in ground motions. We examined the current status of the deep structure of areas in Japan, such as Kanto plain, Osaka plain, Noubi plain, Sendai plain, Niigata plain, etc.

The deep subsurface structure has not been well investigated in Japan.

### Damage and Topography

For the following earthquakes, damage had been presumably caused by the influence of topography. During the Tokachi-oki, 1968 earthquake ( $M=7.8$ ), major damage occurred to the building located along the hill edge, especially in the direction orthogonal to the slope. (Yamahara, 1971) During the Miyagi-ken-oki, 1978 earthquake ( $M=7.4$ ), major damage occurred to the wooden houses built on the alluvial lowland and to

the housing site on reclaimed hilly zone. During the Friuli, Northern Italy, 1976 earthquake ( $M=5.5$ ), major damage occurred at the hilly district on the alluvial fan, at cliff edge, and on the steep hill. (AIJ, 1979) During the Chile earthquake ( $M_s=7.8$ ), a ridge effect is observed at the hilly zone close to the epicenter. (Celebi, 1987) From the Michoacan, 1985 earthquake ( $M_s=8.1$ ), major damage occurred During the Whittier Narrows, 1987 earthquake ( $M_L=5.9$ ), a locally large MMI was observed. There is an analysis which explains the damage due to the irregular soil condition. (Kawase, 1990)

The results of earthquake observation, microtremor measurement, seismic intensity distribution, and damage features are summarized as follows. Cliff is herein defined as the steeper form of slope.

Slope : The dominant frequency and the amplification vary with the height of the hill and the dominant frequency varies with the incident angle of the input motion. The dominant frequency of microtremor and amplitude have good correlation with seismic intensities estimated from questionnaires.

Cliff : It was pointed out by the earthquake observation that amplification becomes larger to the direction orthogonal to the cliff than the horizontally parallel direction to the cliff and the difference becomes less for motion away from the edge. It is also shown that major damage is observed for the direction orthogonal to the cliff.

Mountain (Hill) : It was pointed out from earthquake observation that larger amplification is found at the top of the mountain and the dominant frequency differs between top and skirt of the mountain.

Sediment-filled Valley : It was pointed out from earthquake observation that amplification and dominant frequency varies with the thickness of alluvial deposit, and a surface wave is observed generated from the edge of the valley. These tendency is observed for seismic intensity distribution and the good correlation between thickness of the alluvium and the seismic intensity.

Dipping Base Layer : It was pointed out from earthquake observation that amplification and dominant frequency changes with the depth of overlying layer at the dipping portion, a surface wave is observed generated from the edge of the base layer, and furthermore, dominant frequency at the surface vary with the incident angle at the base layer.

For Deep Subsurface Structure, the followings has been pointed out.

- (1) Surface wave will be generated reflecting the deep subsurface structure of the Kanto plain (basin) due to the shallow earthquake occurring around Kanto plain except for the rather deeper ones. This surface wave holds specific dominant period corresponding to the deep structure of the transmitting path.
- (2) Many researchers support that the propagation of the surface wave is not straight forward from the epicenter to the station, but the propagation or reflection occurs at the edge of the Kanto basin.
- (3) The state of the art on the deep subsurface structure in Kanto plain is not sufficient for the evaluation of design motions for long period building.

## DESCRIPTION OF THE ANALYTICAL MODEL REPRESENTING THE TOPOGRAPHY

The computer analyses were conducted for two sets of representative topographies, i.e., slope and sediment-filled valley. The analytical model for slope came from the existing landform at Kushiro District Meteorological Observatory. Kushiro landform was selected for the analyses. There had been dense earthquake recording arrays and microtremor arrays. There have been comparative earthquake observations after Kushiro earthquake. The geological data around the site is known by the survey on the site.

The two dimensional model of topographies were used for the analyses. The analytical methods used here were finite element method for SV wave, finite difference method and boundary element method for SH wave. The nonlinearity in soil property was not considered in this study. The input motion for the analysis is so called Ricker's wavelet. The result was compared with the result by the one-dimensional propagation model (denoted as 1D hereafter). The comparison was also made for identifying the geographical position showing

larger topographical effect on seismic motion. Further, the degree of simplification in forming the analytical model, the kinds of seismic waves (P-SV, SH waves), influence of impedance ratio and slope angle were also examined by the parametric computations.

### Computational Results for Slope

The models for computer analyses for slope are shown in Fig.2. The model-1 is the realistic model derived from the soil data. The model-2 is the simplified model of model-1 to check the modeling scheme. The model-3 and model-4 are used to check the influence of slope angle and impedance ratio of layers. The dominant frequency of the input motion defined as exposed bedrock motion is 4Hz as shown in Fig.3. For slope model, the incident SH or SV wave is applied to the two dimensional soil model. Comparisons were made between two amplification ratios, one is the ratio between surface response and input motion for two dimensional case (2D hereafter). The other is those for one dimensional model for each location.

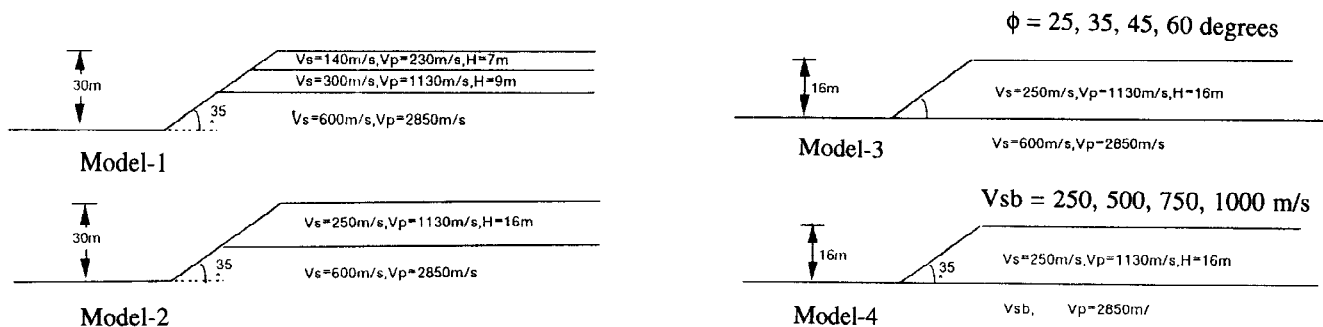


Fig.2 Analytical model for slope

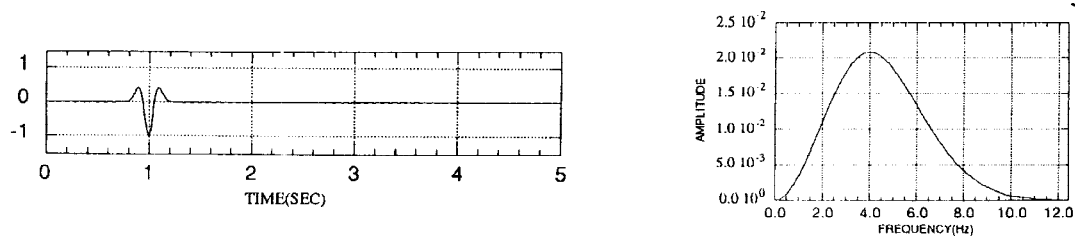


Fig.3 Ricker's wavelet as acceleration input motion at exposed bedrock

Since the influence of slope was found only at the limited portions closer to the lower part of the slope, the comparative study was mainly made for the uphill, the upper part of the hill. The analytical methods used here are 2-dimensional FEM and BEM. We had acknowledged rough coincidence between the computational results for two methods. Figure 4 shows the spatial distribution of transfer functions of model-1 for SH and SV wave incidence cases together with 1D case. The difference in transfer function is larger for portions closer to the slope edge and becomes smaller for distances away from the edge. When using the simplified model-2, a similar tendency with model-1 is observed in Fig.5. Two transfer functions for model-1 and model-2 is compared in Fig.6 for SV. This difference is caused by the model simplification. The result shows that the modeling scheme has an influence on the transfer function. When the transfer function is normalized with the corresponding transfer function with the 1D basis (denoted as normalized transfer function hereafter), the difference of two normalized transfer function becomes smaller as shown in Fig.7. The ground response at the upper part of the hill consists of two types of waves, i.e., the body wave propagating from the lower layer, and the wave propagating horizontally from the slope. The latter can be recognized as separate wave from portions much away from the edge. This wave is called a later phase (wave). The propagation velocity for the later phase is the phase velocity of the Love wave for the SH wave incidence, and the phase velocity of the Rayleigh wave for the SV wave incidence. Or, the later phase generated at the edge of each topography is

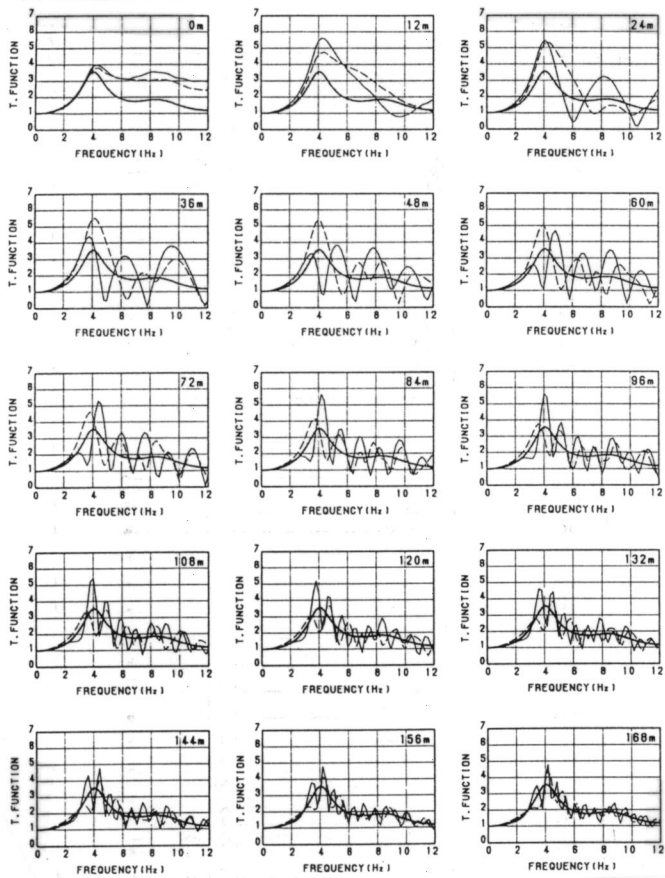


Fig.4 Spatial distribution of transfer functions for Model-1 — 1D, — SH, - - - SV

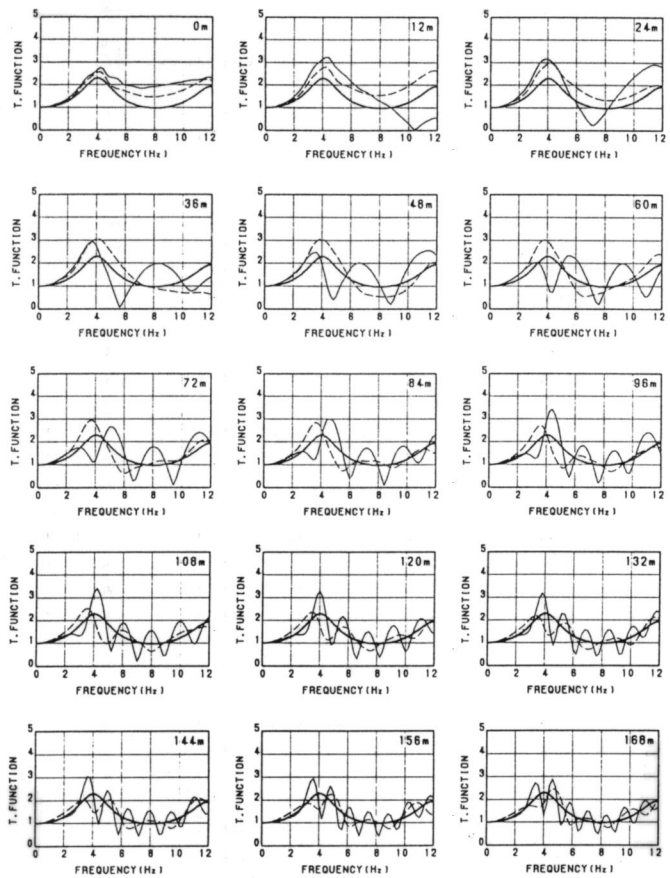


Fig.5 Spatial distribution of transfer functions for Model-2 — 1D, — SH, - - - SV

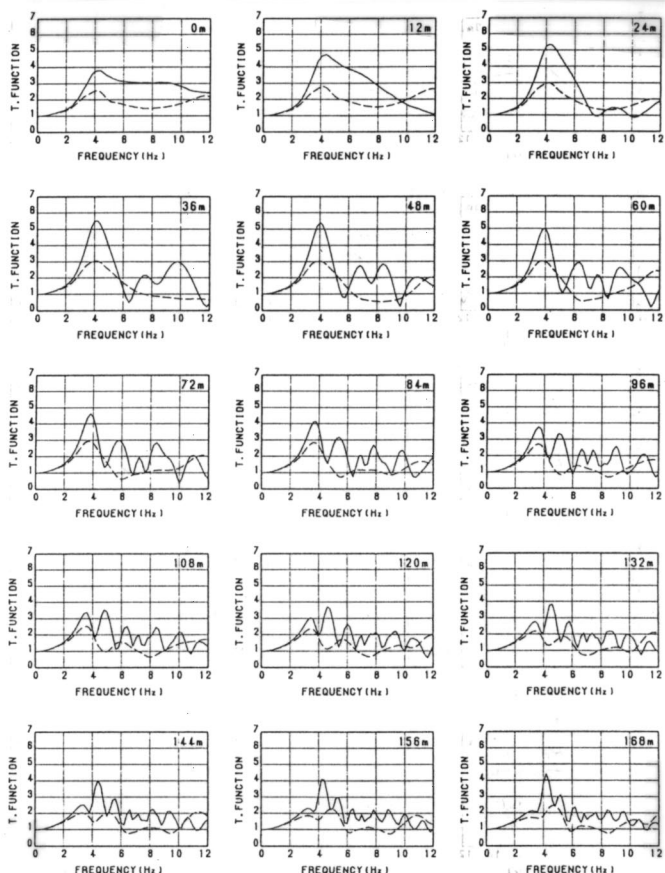


Fig.6 Spatial distribution of transfer functions for Model-1 and Model-2 — Model-1, - - - Model-2

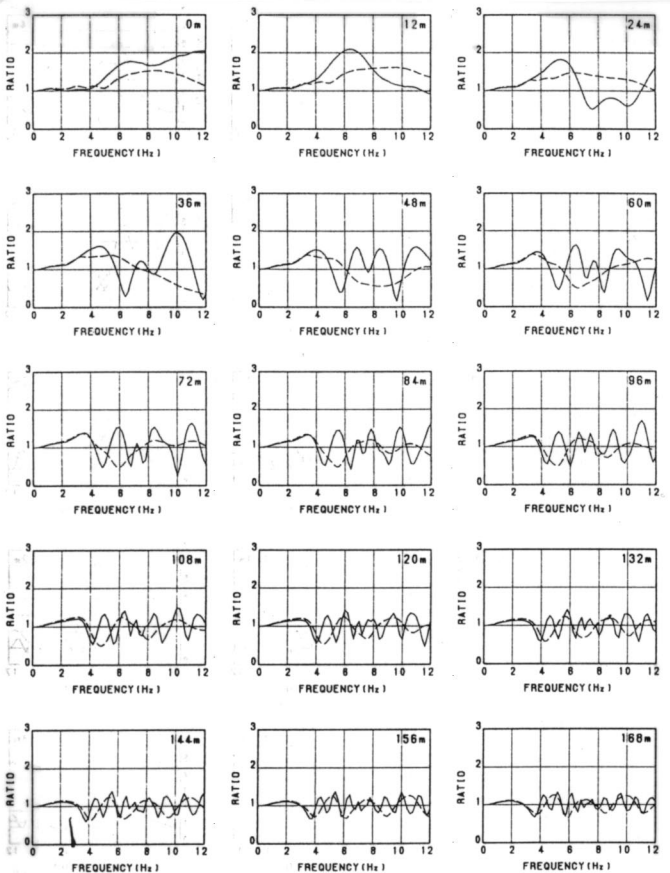


Fig.7 Spatial distribution of normalized transfer functions for Model-1 and Model-2 — Model-1, - - - Model-2

dominated with surface wave. For portion away from the edge, the generated later phase will be attenuated, and there might be small difference in amplification compared with the amplification from 1D basis. It is seen from the analysis using SH and SV, that the peak frequency of the transfer function is 3.5 to 6 Hz. The maximum amplitudes of the computed responses fluctuate along the hilltop. The maximum transfer function occurs at 18 and 100 meters from the edge for SH case, and at 40 meters for SV case. The maximum amplitude in time history occurs at about 10 meters from the edge for SH wave incidence, and at 20 meters from the edge for SV wave incidence. The maximum amplitude approximately 1.5 times larger than the one for 1D case. The influence of the different propagating velocity of the later phase is more apparent in SH wave incidence than in SV wave incidence for larger amplitude variation.

The influences of slope angle upon the normalized transfer function and the maximum amplitude in time domain are shown in Fig.8 and Fig.9, respectively. The influence of slope angle ranging 25 to 60 degrees becomes larger in transfer function for the closer to the edge and for higher frequency. However, there is a small influence of slope angle in both of transfer function and time domain response.

The maximum amplitudes of ground responses in reference with the results of 1D results are shown in Fig.10 for 4 cases of impedance ratios. It is seen from the figure that the influence of impedance ratio is relatively small.

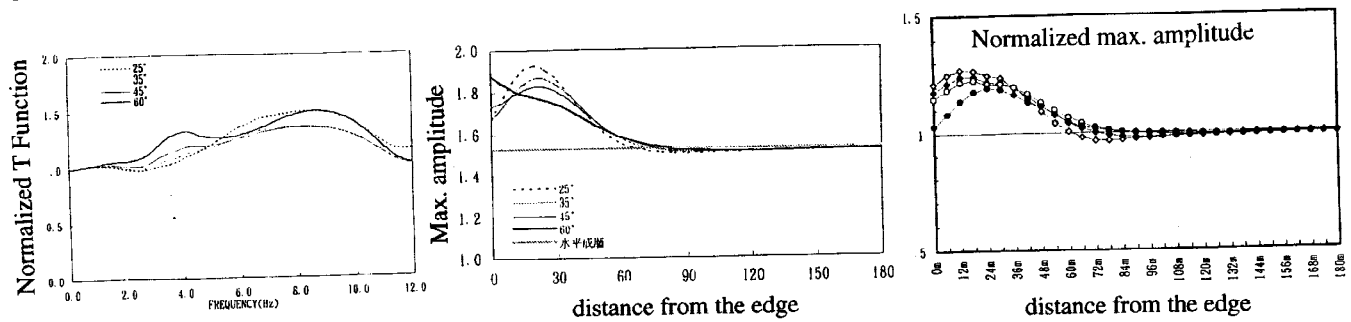


Fig.8 Normalized transfer function Fig.9 Maximum amplitude Fig.10 Normalized maximum amplitude

Computational Results for Sediment-filled Valley

The analytical model for sediment-filled valley is shown in Fig.11 The variations of the models are summarized in Table 2 The model is symmetrical. The shapes of the models were determined with reference of actual landforms and considering the frequency content, number of elements, dimension of element, computation efficiency. These model is basically constructed as two dimensional half space with trapezoidal alluvial deposit. The impedance ratio between two deposit is assigned as 3 for standard case. The Ricker's wavelet is also used as input motion for this case, however, the dominant frequency is 2.17 Hz and the peak amplitude occurs at 1.5 second from the beginning in the time domain as shown in Fig.12. The analytical methods used are finite difference method and boundary element method for SH wave incidence cases and finite element method is used for SV incidence case. The division of elements was made so that we may discuss the dynamic properties less than 10 Hz.

Table 2 Analytical model of sediment-filled valley

	Sediment-filled Valley			Bedrock	
	width (m)	depth (m)	side inclination (deg)	side boundary (m)	lower boundary (m)
Model-A	200	15	45	200	75
Model-B	100	15	45	200	75
Model-C	50	15	45	200	75

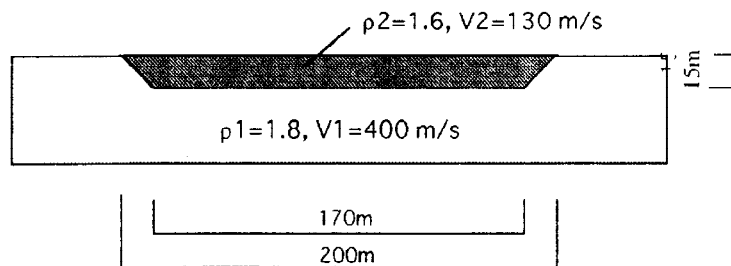


Fig.11 Analytical model of sediment-filled valley for Model-A

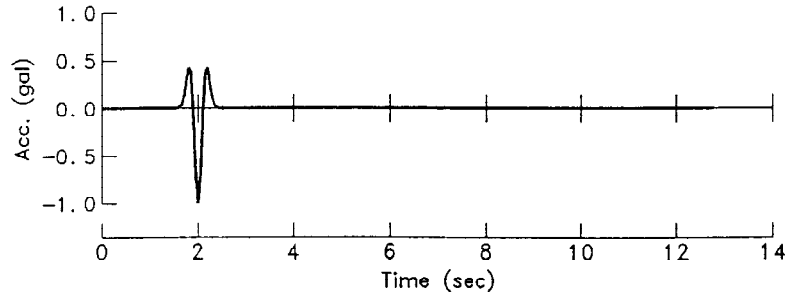


Fig.12 Ricker's wavelet as acceleration input motion at exposed bedrock

horizontal length of the valley. It is seen from Fig.13 that the secondary surface wave generated at the edge of the valley propagates in horizontal direction, and repeats reflection, gradually attenuates. The overlapping of waves changes the pattern of distribution of peak values. As valley becomes narrow, the peak amplitude tends to take its largest at the middle point of the valley. The transfer functions for 1D and 2D cases are compared at several points of the surface. The fluctuation of the transfer function with frequency is large when the damping is smaller. When the damping is larger, however, the transfer functions for both cases become smoother and are comparable each other at points away from the dipping base. For areas close to the edge of the valley, the difference becomes eminent. For cases with narrower valley, the influence of the valley edge extends to the closer point to the valley edge.

## CONCLUSIONS

The typical site conditions in urban area considering the irregularity in topography was surveyed. The topographically irregular soil conditions in urban area in Japan are specified and represented with dimension of landform, angle of slope, distance from the edge, etc. The spatial variation of ground motion properties such as max. amplitudes, transfer function and predominant periods are computed for each of cases.

## ACKNOWLEDGMENT

This research has been implemented as part of the research project of the Ministry of Construction, Government of Japan. For the project, a research committee (Chairman : Dr. Tadao Minami, Professor of the University of Tokyo) was organized in the Japan Institute of Construction Engineering (JICE). Under the auspices of the committee, a working group (Head : Dr. Kazuo Seo, Professor of Tokyo Institute of Technology) was organized. The literature survey, model formation and computations were conducted by the members of working group. The authors belong to the working group. We express heartfelt thanks to the members of the committee and the working group for advises and collaboration.

## REFERENCES

AIJ (1987). Reconnaissance Report of 1985 Mexico Earthquake, (in Japanese)  
 BRI and BCJ (1992). A Guideline for Composing Design Earthquake Ground Motion for Dynamic Analysis of Buildings, *Appendix of Annual Report of the Committee on Technical Guideline for Design Earthquake Ground Motion*  
 BRI, JICE (1993). Annual Report of the Project for 1992 fiscal year, (in Japanese)  
 BRI, JICE (1994). Annual Report of the Project for 1993 fiscal year, (in Japanese)  
 Celebi, M., (1987). Topographical and Geological Amplifications Determined from Strong-Motion and Aftershock Records of the 3 March 1985 Chile earthquake, *B.S.S.A.*, **77**, 1147-1167  
 Kawase, H. (1990). Topography effect at the critical SV-wave incidence: Possible Explanation of Damage Pattern by the Whittier Narrows, California earthquake of 1 October 1987, *B.S.S.A.*, **80**, pp.1-22  
 Yamahara, H., (1971). Soils and School, *Planning of School Building*, AIJ, (in Japanese)

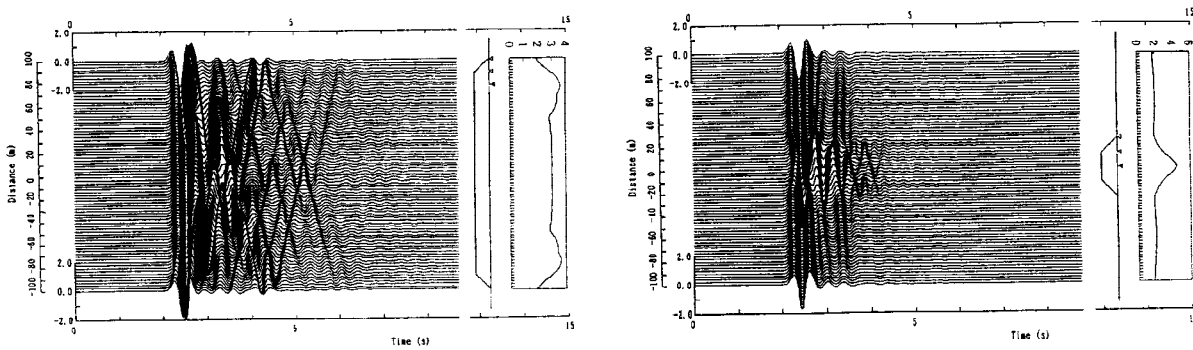


Fig.13 Response waveform at the surface and the distribution of maxima for Model-A and Model-C

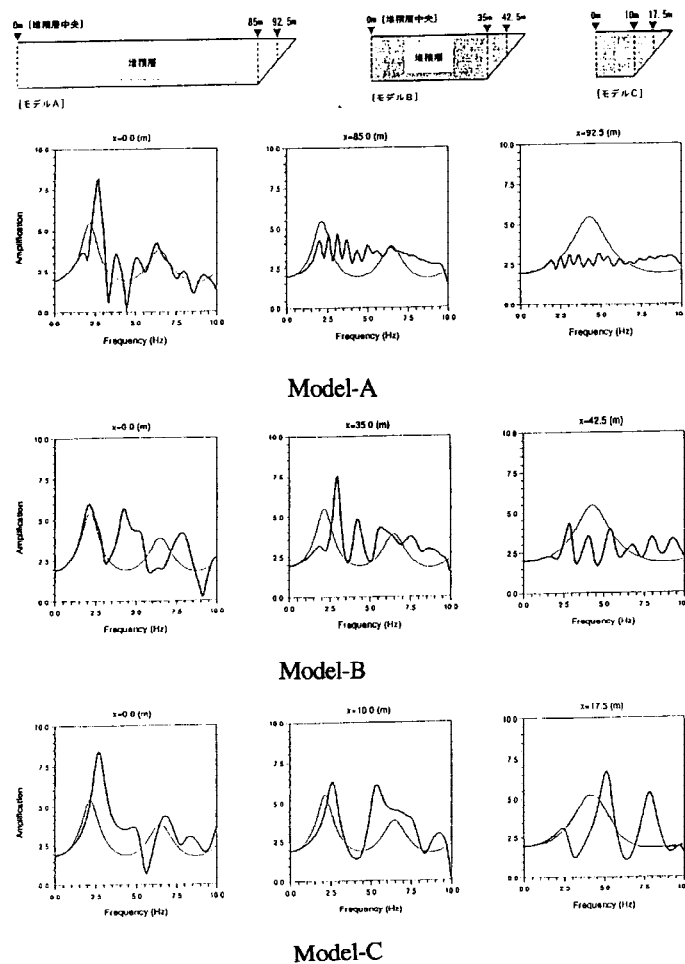


Fig.14 Comparison of transfer functions for three models with 1D case